

Microbiology and Immunology

First published: 16 December 2019

DOI : 10.1111/1348-0421.12766

***In vitro* vRNA–vRNA interactions in the H1N1 influenza A virus genome**

インフルエンザウイルスの
ゲノム分節間相互作用の解析

宮本 翔

This is the peer-reviewed version of the following article: “Miyamoto, S., and Noda, T. *In vitro* vRNA–vRNA interactions in the H1N1 influenza A virus genome. *Microbiology and Immunology*. 2019”, which has been published in final form at <https://doi.org/10.1111/1348-0421.12766>. This article may be used for non-commercial purposes in accordance with Wiley Terms and Conditions for the Use of Self-Archived Versions.

Sho Miyamoto ORCID iD: 0000-0001-6541-1722

Takeshi Noda ORCID iD: 0000-0002-0658-4663

Original Article

Subject section: Virology

Specific field: Animal RNA virus

***In vitro* vRNA–vRNA interactions in the H1N1 influenza A virus genome**

Running title: Inter-segment interactions in the influenza A virus genome

Sho Miyamoto^{a,b} and Takeshi Noda^{a,c,*}

^a Laboratory of Ultrastructural Virology, Institute for Frontier Life and Medical Sciences, Kyoto University, 53 Shogoin Kawahara-cho, Sakyo-ku, Kyoto 606-8507, Japan

This article has been accepted for publication and undergone full peer review but has not been through the copyediting, typesetting, pagination and proofreading process, which may lead to differences between this version and the Version of Record. Please cite this article as doi: 10.1111/1348-0421.12766.

This article is protected by copyright. All rights reserved.

^b Department of Molecular Virology, Graduate School of Medicine, Kyoto University, 53 Shogoin Kawahara-cho, Sakyo-ku, Kyoto 606-8507, Japan

^c Laboratory of Ultrastructural Virology, Graduate School of Biostudies, Kyoto University, 53 Shogoin Kawahara-cho, Sakyo-ku, Kyoto 606-8507, Japan

* **Corresponding author:**

Takeshi Noda

Laboratory of Ultrastructural Virology, Institute for Frontier Life and Medical Sciences, Kyoto University, 53 Shogoin Kawahara-cho, Sakyo-ku, Kyoto 606-8507, Japan

Phone: +81-75-751-4019

E-mail: t-noda@infront.kyoto-u.ac.jp

Abstract

The genome of influenza A virus consists of eight-segmented, single-stranded, negative-sense viral RNAs (vRNAs). Each vRNA contains a central coding region that is flanked by noncoding regions. It has been shown that upon virion formation,

the eight vRNAs are selectively packaged into progeny virions through segment-specific packaging signals that are located in both the terminal coding regions and adjacent noncoding regions of each vRNA. Although recent studies using next generation sequencing suggest that multiple inter-segment interactions are involved in genome packaging, contributions of the packaging signals to the inter-segment interactions are not fully understood. Herein, using synthesized full-length vRNAs of H1N1 WSN virus and short vRNAs containing the packaging signal sequences, we performed *in vitro* RNA binding assays and identified 15 inter-segment interactions among eight vRNAs, most of which were mediated by the 3'- and 5'-terminal regions. Interestingly, all eight vRNAs interacted with multiple other vRNAs, in that some bound to different vRNAs through their respective 3'- and 5'-terminal regions. These *in vitro* findings would be of use in future studies of *in vivo* vRNA-vRNA interactions during selective genome packaging.

Keywords:

Genome packaging signal, Influenza A virus, inter-segment interaction, *in vitro* vRNA–vRNA interaction, selective genome packaging

1. Introduction

The genome of influenza A virus consists of eight segmented, single-stranded, negative-sense RNAs (vRNAs). Each contains a central coding region in the antisense orientation flanked by segment-specific noncoding and common terminal promoter regions. The vRNAs are associated with multiple nucleoproteins (NPs) and a heterotrimeric viral RNA-dependent RNA polymerase complex composed of PB2, PB1, and PA proteins, resulting in the formation of a helical, rod-shaped ribonucleoprotein complex (vRNP). The vRNP is responsible for transcription and replication of constituent vRNAs and the incorporation of vRNAs into progeny virions. Recent studies show that NPs, in the context of vRNPs, bind to vRNAs non-uniformly without sequence specificity (1, 2). Importantly, next-generation sequencing analyses have demonstrated that some regions of the vRNAs, in the context of vRNPs, are free of NPs and able to form secondary or tertiary structures on the surface of the rod-shaped vRNPs (3).

It has been demonstrated that progeny virions selectively package a single copy of each of the eight vRNAs. The eight vRNAs, in the form of vRNPs, are arranged in a specific 1+7 pattern within the virion, in which one central vRNP is

surrounded by the other seven vRNPs (4, 5). Although mechanisms underlying genome packaging are not fully understood, it has been well-documented that segment-specific packaging signal sequences play critical roles in packaging (6-11). The segment-specific packaging signal of each vRNA is bipartite, located in both the terminal coding regions and adjacent noncoding regions, comprising up to 300 nucleotides. The terminal coding regions within the packaging signal are important for the co-packaging of multiple vRNAs and are referred to as bundling signals (12). Mutations or deletions in the bundling signal of a particular vRNA reduce the packaging efficiencies of not only that vRNA, but also of the other vRNAs. The effects of such mutations or deletions on packaging efficiency is hierarchical among the eight vRNAs, with PB2 vRNA having the greatest effect on the packaging of the other vRNAs (8, 13-20). Accordingly, it has been proposed that there are functional interactions among the eight vRNAs through the genome packaging signals that direct selective genome packaging.

Previously, vRNA–vRNA interactions among eight distinct vRNAs were analyzed by *in vitro* RNA binding assays for human H3N2 and avian H5N2 viruses using vRNAs synthesized *in vitro* (21, 22). This strategy has limited efficacy, as it is unknown whether all *in vitro* interactions take place within the viral particles and

infected cells (23). Nevertheless, these studies identified an *in vitro* interaction between PB1 and NA vRNAs of both the H3N2 and H5N2 viruses. Importantly, the finding was confirmed by virological experiments, which confirmed that PB1 and NA vRNAs are efficiently co-packaged into progeny virions (3, 24, 25). This evidence provides a basis for *in vitro* RNA binding assays in identifying possible vRNA–vRNA interactions in the context of vRNPs.

Nevertheless, our knowledge of vRNA–vRNA interactions of the H1N1 genome is still lacking. To expand understanding of the molecular mechanism of genome packaging, studies of inter-segment interactions of various subtypes are necessary.

Here, to understand *in vitro* vRNA-vRNA interactions of the H1N1 virus, we performed *in vitro* RNA binding assays for H1N1 WSN (A/WSN/33) genome segments, using both full-length vRNAs and short vRNAs containing the segment-specific genome packaging signal sequences.

2. Materials and Methods

2.1. *In vitro* RNA synthesis

Full-length and short vRNAs were synthesized *in vitro* using T7 transcription as described previously (26). Briefly, templates containing a T7 phage promoter sequence (5'-TAATACGACTCACTATAGGG-3') were amplified by PCR using corresponding primer pairs and purified with the QIAquick PCR purification kit (Qiagen, Hilden, Germany). PCR primers are listed in Tables S1 and S2. Pol I plasmids containing cDNA sequences of either A/WSN/33 (H1N1) and A/Udorn/307/72 (H3N2) viral genes (27) were used as templates. The purified PCR products were transcribed *in vitro* using the RiboMAX Large Scale RNA Production System-T7 (Promega, Madison, WI) at 37 °C for 4 h, followed by RQ1 DNase I (Promega) treatment for digestion of the DNA template at 37 °C for 15 min. Transcripts were purified using the RNeasy Mini Kit (Qiagen).

2.2. *In vitro* RNA binding assay

RNA–RNA interactions were evaluated by electrophoretic mobility shift assays using conventional protocols (28-31). Pairs of purified vRNAs (2 pmol of each) were denatured for 10 min at 65 °C in 5 µL of ultrapure water and cooled on

ice. Thereafter, 5 μL of 2-fold concentrated buffer (final concentration: 50 mM HEPES, 50 mM KCl, and 20 mM MgCl_2) was added and samples were incubated for 2 h at 37 °C. Then, 2 μL of loading buffer [40% (v/v) glycerol and 0.05% (w/v) bromophenol blue] was added to the samples and they were electrophoresed on 1% agarose gels containing 0.01% (w/v) ethidium bromide. Native gel electrophoresis of the RNA complexes was performed at 4 °C in a buffer containing 50 mM Tris, 44.5 mM borate, and 0.1 mM MgCl_2 . The RNA weight fraction (%) of each band in each lane was measured by Image LabTM (Bio-rad, Richmond, CA). Percentage of RNA–RNA complexes were determined by dividing the weight fraction of the corresponding band by the sum of the weight fractions of all the bands in that lane (21). For analyses using short vRNAs, we performed the experiments in the same way as described above except that samples were incubated for 30 min at 37 °C and electrophoresed on a 2% agarose gel.

2.3. Statistical analysis

Statistical analyses were performed in R (32). The proportions of heterodimers were compared to those of homodimers of M vRNA using one-way ANOVA with Dunnett's test. A value of $P < 0.05$ was considered to be significant.

2.4. *in silico* analysis of RNA-RNA interactions

RNA-RNA interactions were predicted by RNAcofold software in the ViennaRNA package 2.0 (33). Correlations between the minimal free energies and the proportions of heterodimers were analyzed by Pearson correlation.

3. Results

3.1. Experimental conditions for *in vitro* RNA binding assays of H1N1 WSN vRNAs

Although *in vitro* vRNA–vRNA interactions have been reported for H3N2 and H5N2 viruses, there are no such reports for H1N1. To identify *in vitro* vRNA-vRNA interactions among the eight vRNAs of H1N1 WSN virus, we performed *in vitro* RNA binding assays using synthesized full-length vRNAs as reported previously (21, 22) with some modifications. Because the interaction between NA and PB1 vRNAs is consistently detected for H3N2 and H5N2 viruses, we began by analyzing full-length NA and PB1 vRNAs of the H1N1 WSN virus to set the proper experimental conditions for detecting other vRNA–vRNA interactions for H1N1.

As shown in Figure 1, in the presence of more than 8 mM MgCl₂, the divalent cation of which is known to be responsible for the tertiary structure formation in RNAs (34, 35), the H3N2 Udorn PB1–NA vRNA complex was detected as expected. Similarly, the PB1–NA complex was detected for H1N1 WSN, requiring MgCl₂, suggesting the necessary requirement of Mg²⁺ for detecting vRNA–vRNA interactions. These results are consistent with those from previous studies showing that NA vRNA is co-packaged with PB1 vRNA into progeny virions in both H1N1 PR8 and H3N2 Udorn viruses (24, 25). In contrast, HA and M vRNAs of the H1N1 WSN virus did not form a complex even when the concentration of MgCl₂ was increased (Fig. 1b), supporting a specific interaction between H1N1 WSN PB1 and NA vRNAs. Hence, we performed H1N1 WSN RNA binding assays in the presence of 20 mM MgCl₂.

3.2. *In vitro* inter-segment interactions among full-length H1N1 WSN vRNAs

Next, we analyzed all possible H1N1 WSN vRNA combinations (Figs. 2 and S1). When individual full-length vRNAs were incubated singly, they formed homodimers inefficiently; at the most, only 18% M vRNA was found in homodimers (Fig. 2b). In contrast, several pairs of vRNAs efficiently formed

heterodimers; for example, 48% of PB1 and NA vRNAs and 55% of HA and NA vRNAs formed heterodimers (Fig. 2b). Among the 28 possible vRNA pairings, we identified 13 (PB2–HA, PB2–NS, PB1–HA, PB1–NA, PB1–M, PB1–NS, PA–HA, PA–NS, HA–NA, HA–NS, NP–NA, NP–M, and NP–NS) for which heterodimer formation was significantly greater than that for M vRNA alone (Fig. 2b, shown in gray). Among the 13 combinations, inter-segment interactions between PB1 and NA, and NP and NS have also been reported for both the H3N2 and H5N2 viruses (21, 22), whereas PB2–HA, PB2–NS, PB1–M, and HA–NA vRNAs were unique to H1N1 WSN, although their experimental conditions were different from ours. Interestingly, all eight vRNAs showed interactions with multiple partner vRNAs; for example, HA vRNA interacted with PB2, PB1, PA, NA, and NS vRNAs, while PB2 vRNA formed heterodimers with HA and NS vRNAs, suggesting that each vRNA contains multiple interacting regions.

3.3. *In vitro* vRNA–vRNA interactions through the terminal regions containing genome packaging signals

Although all eight vRNAs interacted with multiple other vRNAs in our *in vitro* assay, PB2 and PA vRNAs had fewer partners than the others (Fig. 2b). The

PB2, PB1 and PA vRNAs are essential for selective genome packaging; the deletion of any of these three causes a large reduction in the packaging of other vRNAs (8, 20). This discrepancy may be due to a technical issue with the *in vitro* RNA binding assay, as RNAs longer than a few hundred nucleotides fail to fold to produce the functional secondary or tertiary structures required for RNA-RNA interactions (36-39). To circumvent this theoretical problem and to further decipher the contribution of the genome packaging signal to local inter-segment interactions, we prepared 16 short vRNAs comprised of a noncoding region and an adjacent coding region with 120–300 nucleotides, containing either the 3'- or 5'-end of the genome packaging signal (Fig. 3a). We used the lengths of each segment's genome packaging regions reported by Muramoto et al. (8), although the exact lengths of the genome packaging signal regions have yet to be determined. All 13 combinations of the identified inter-segment interactions presented in Figure 2b, as well as pairs among PB2, PB1, and PA (PB2–PB1, PB2–PA, and PB1–PA) were analyzed using these short vRNAs (Figs. 3b, 3c, 3d, and S2). 11 of the 13 combinations, excluding the PB2–NS and NP–NA pairs, showed efficient heterodimer formation, suggesting the importance of the genome packaging signal regions for inter-segment interactions. Although heterodimer formation was not

detected for the PB2–PA or PB1–PA combinations when full-length vRNAs were used, heterodimers of 5'PB2(300)–5'PA(180), 5'PB1(240)–5'PA(180), 3'PB1(240)–3'PA(180), 5'PA(180)–3'PB2(300), and 3'PB1(240)–5'PA(180) were detected using the short vRNAs. Interestingly, some vRNAs are associated with different vRNAs through the 3'- and 5'-ends of their terminal regions; the 5'-HA interacted with PB2 and PB1 vRNA, whereas the 3'-HA interacted with PB2, PA, NA, and NS vRNAs.

Finally, we analyzed the minimal free energies of respective pairs of vRNAs *in silico* using RNAcofold (33) (Figs. S3a, S3b, and S3c). Interestingly, the minimal free energies for interactions of pairs of vRNA fragments were significantly correlated with our *in vitro* RNA-RNA interaction data (Fig. S3d, Pearson correlation coefficient $R = -0.56$, $p < 0.001$). In addition, combinations of vRNAs which showed interactions in our *in vitro* assays showed lower free energies (Mean = -11.9 ± 4.0 kcal/mol; Student's *t*-test $p < 0.001$) compared to interaction-negative combinations of vRNAs (Mean = -8.6 ± 3.3 kcal/mol), supporting the applicability of *in vitro* RNA binding assays for the identification of such *in vitro* interactions.

4. Discussion

Specific inter-segment interactions are believed to be required for accurate packaging of the eight vRNAs of influenza A viruses. In this study, we prepared *in vitro*-transcribed vRNAs of the H1N1 WSN virus and performed *in vitro* RNA binding assays. We showed *in vitro* vRNA-vRNA interactions among the eight vRNAs through terminal regions containing genome packaging signals, and all eight vRNAs may interact with multiple vRNAs.

In our *in vitro* H1N1 WSN RNA binding assays, we showed 15 inter-segment interactions (Figs. 2 and 3) in which two combinations were the same as previously reported for the H3N2 and H5N2 viruses (21, 22), and six were unique to the H1N1 WSN virus. These results suggest that some pairings, including PB1-NA and NP-NS vRNAs, would be conserved among multiple HA subtypes of influenza A viruses, whereas many pairings might be unique to the particular strains or HA subtypes. This is consistent with the results of previous studies using H3N2 and H5N2, in which different combinations of inter-segment interactions were observed, except for PB1-NA and NP-NS vRNAs interactions (21, 22), although these results cannot be directly compared due to different experimental

conditions. Therefore, the study and identification of vRNA–vRNA interactions of additional HA subtypes of influenza A viruses are needed for further understanding the mechanisms of selective genome packaging.

Considering that the sequence of NA vRNA of H1N1 WSN is substantially different from those of H3N2 (A/Moscow/10/1999) and H5N2 (A/Finch/England/2051/1991) (46.9 and 46.5 % identity at the nucleotide level, respectively) (21, 22) but that of PB1 vRNA of H1N1 WSN virus is more relatively similar to H3N2 and H5N2 (82.7 and 83.4%, respectively), it was interesting to note that the intersegment interaction between PB1 and NA vRNAs is conserved in the N1 and N2 subtypes. Although there is a report that nucleotides 1776 to 2070 of PB1 vRNA are involved in the interaction with N2NA (25), the mechanism through which this region in PB1 vRNA interacts with different sequences of N1NA and N2NA remains unclear. Our *in vitro* study showed a direct interaction of N1NA with PB1 vRNAs in H1N1 WSN virus mediated by local interactions of its 5' terminal region with the 3' and 5' terminal regions of the PB1 vRNA. Thus, multiple interactions between NA and PB1 vRNAs may be involved in co-packaging of NA and PB1 vRNAs (3).

Because we used *in vitro*-transcribed vRNAs for the *in vitro* RNA binding assays, their secondary and tertiary structures are likely different from those they would adopt when part of vRNPs *in vivo*. Accordingly, it should be noted that interactions identified by *in vitro* RNA binding assays do not necessarily reflect interactions in the context of vRNPs. In our *in vitro* RNA binding assay, we employed a relatively higher concentration of Mg^{2+} (20 mM), since we did not detect stable interactions between two RNA segments under physiological conditions in cells (<5mM) (Fig. 1). This requirement is likely because naked RNAs generally do not fold into active structures under physiological conditions *in vitro* by themselves (30). The manifestation of RNA activity under physiological conditions requires protein cofactors in most cases (40). Therefore, it is possible that stable vRNA-vRNA interactions require host- and/or viral- proteins such as viral NPs. Further studies are needed to reveal whether such *in vitro* interactions are maintained when vRNAs are in the form of vRNPs and whether they are involved in selective genome packaging.

We found that all eight vRNAs interact with multiple other vRNAs *in vitro*, primarily through their terminal regions containing genome packaging signals (Figs. 2 and 3). We also demonstrated that some vRNAs interact with others

through the 3'- and 5'-ends of their terminal regions. Moreover, some of these termini contain multiple regions that can interact with other vRNAs (Fig. 3). This is consistent with recent SHAPE-MaP and SPLASH analyses of vRNAs within virions, in which each vRNA interacts with multiple vRNAs not only through packaging signal regions but also through central coding regions (3), supporting the notion that each vRNA has multiple interactions during genome packaging. However, it is difficult to expect that a particular vRNA interacts with more than three vRNAs simultaneously if it is not located in the center of the 1+7 arrangement of eight vRNPs during the genome packaging process (41). Although our *in vitro* results indicate that PB1 and HA vRNAs potentially interact with five other vRNAs (Fig. 3), all of these interactions might not arise in the context of virus replication in cells.

In conclusion, we demonstrated *in vitro* inter-segment interactions of H1N1 WSN virus genome segments through their terminal regions, which contain the genome packaging signals. Although further studies are needed to evaluate the identified interactions in the context of virus replication, understanding inter-segment interactions in multiple HA subtypes of influenza A virus will contribute to the elucidation of selective genome packaging mechanisms and to

improved prediction of the emergence of reassortant influenza A viruses with potential for causing pandemics.

Acknowledgements

We thank Connor Park for editing the manuscript. This work was supported by JSPS KAKENHI Grant JP19J14928 (to S.M.), JSPS Grant-in-Aid for Scientific Research (B) (17H04082), JSPS Grant-in-Aid for Challenging Research (Exploratory) (19K22529), the JSPS Core-to-Core Program A, the Advanced Research Networks, MEXT Grant-in-Aid for Scientific Research on Innovative Area (19H04831), AMED Research Program on Emerging and Re-emerging Infectious Diseases (18fk0108055h0002), AMED Japanese Initiative for Progress of Research on Infectious Disease for global Epidemic (18fm0208003h0002), the Grant for Joint Research Project of the Institute of Medical Science, University of Tokyo, the Joint Usage/Research Center program of Institute for Frontier Life and Medical Sciences Kyoto University, the Daiichi Sankyo Foundation of Life Science, and the Takeda Science Foundation (to T.N.).

Disclosure:

The authors declare no competing interests.

This article is protected by copyright. All rights reserved.

References

1. Lee N, Le Sage V, Nanni AV, Snyder DJ, Cooper VS, Lakdawala SS. Genome-wide analysis of influenza viral RNA and nucleoprotein association. *Nucleic Acids Research*. 2017;45(15):8968-77.
2. Williams GD, Townsend D, Wylie KM, Kim PJ, Amarasinghe GK, Kutluay SB, Boon ACM. Nucleotide resolution mapping of influenza A virus nucleoprotein-RNA interactions reveals RNA features required for replication. *Nat Commun*. 2018;9(1):465.
3. Dadonaite B, Gilbertson B, Knight ML, Trifkovic S, Rockman S, Laederach A, Brown LE, Fodor E, Bauer DLV. The structure of the influenza A virus genome. *Nature microbiology*. 2019;4(11):1781-9.
4. Noda T, Sagara H, Yen A, Takada A, Kida H, Cheng RH, Kawaoka Y. Architecture of ribonucleoprotein complexes in influenza A virus particles. *Nature*. 2006;439(7075):490-2.

5. Chou YY, Vafabakhsh R, Doganay S, Gao Q, Ha T, Palese P. One influenza virus particle packages eight unique viral RNAs as shown by FISH analysis. *Proc Natl Acad Sci U S A*. 2012;109(23):9101-6.
6. Fujii K, Fujii Y, Noda T, Muramoto Y, Watanabe T, Takada A, Goto H, Horimoto T, Kawaoka Y. Importance of both the coding and the segment-specific noncoding regions of the influenza A virus NS segment for its efficient incorporation into virions. *Journal of virology*. 2005;79(6):3766-74.
7. Fujii Y, Goto H, Watanabe T, Yoshida T, Kawaoka Y. Selective incorporation of influenza virus RNA segments into virions. *Proc Natl Acad Sci U S A*. 2003;100(4):2002-7.
8. Muramoto Y, Takada A, Fujii K, Noda T, Iwatsuki-Horimoto K, Watanabe S, Horimoto T, Kida H, Kawaoka Y. Hierarchy among viral RNA (vRNA) segments in their role in vRNA incorporation into influenza A virions. *Journal of virology*. 2006;80(5):2318-25.
9. Ozawa M, Fujii K, Muramoto Y, Yamada S, Yamayoshi S, Takada A, Goto H, Horimoto T, Kawaoka Y. Contributions of two nuclear localization signals of

influenza A virus nucleoprotein to viral replication. *Journal of virology*.

2007;81(1):30-41.

10. Ozawa M, Maeda J, Iwatsuki-Horimoto K, Watanabe S, Goto H, Horimoto T, Kawaoka Y. Nucleotide sequence requirements at the 5' end of the influenza A virus M RNA segment for efficient virus replication. *Journal of virology*.

2009;83(7):3384-8.

11. Watanabe T, Watanabe S, Noda T, Fujii Y, Kawaoka Y. Exploitation of nucleic acid packaging signals to generate a novel influenza virus-based vector stably expressing two foreign genes. *Journal of virology*. 2003;77(19):10575-83.

12. Goto H, Muramoto Y, Noda T, Kawaoka Y. The genome-packaging signal of the influenza A virus genome comprises a genome incorporation signal and a genome-bundling signal. *Journal of virology*. 2013;87(21):11316-22.

13. Gao Q, Chou YY, Doganay S, Vafabakhsh R, Ha T, Palese P. The influenza A virus PB2, PA, NP, and M segments play a pivotal role during genome packaging. *Journal of virology*. 2012;86(13):7043-51.

14. Gog JR, Afonso Edos S, Dalton RM, Leclercq I, Tiley L, Elton D, von Kirchbach JC, Naffakh N, Escriou N, Digard P. Codon conservation in the influenza A virus genome defines RNA packaging signals. *Nucleic Acids Res.* 2007;35(6):1897-907.
15. Hutchinson EC, Curran MD, Read EK, Gog JR, Digard P. Mutational analysis of cis-acting RNA signals in segment 7 of influenza A virus. *Journal of virology.* 2008;82(23):11869-79.
16. Hutchinson EC, Wise HM, Kudryavtseva K, Curran MD, Digard P. Characterisation of influenza A viruses with mutations in segment 5 packaging signals. *Vaccine.* 2009;27(45):6270-5.
17. Liang Y, Hong Y, Parslow TG. cis-Acting packaging signals in the influenza virus PB1, PB2, and PA genomic RNA segments. *Journal of virology.* 2005;79(16):10348-55.
18. Liang Y, Huang T, Ly H, Parslow TG, Liang Y. Mutational analyses of packaging signals in influenza virus PA, PB1, and PB2 genomic RNA segments. *Journal of virology.* 2008;82(1):229-36.

19. Marsh GA, Hatami R, Palese P. Specific residues of the influenza A virus hemagglutinin viral RNA are important for efficient packaging into budding virions. *Journal of virology*. 2007;81(18):9727-36.
20. Marsh GA, Rabadan R, Levine AJ, Palese P. Highly conserved regions of influenza a virus polymerase gene segments are critical for efficient viral RNA packaging. *Journal of virology*. 2008;82(5):2295-304.
21. Fournier E, Moules V, Essere B, Paillart JC, Sirbat JD, Isel C, Cavalier A, Rolland JP, Thomas D, Lina B, Marquet R. A supramolecular assembly formed by influenza A virus genomic RNA segments. *Nucleic Acids Res*. 2012;40(5):2197-209.
22. Gavazzi C, Isel C, Fournier E, Moules V, Cavalier A, Thomas D, Lina B, Marquet R. An in vitro network of intermolecular interactions between viral RNA segments of an avian H5N2 influenza A virus: comparison with a human H3N2 virus. *Nucleic Acids Res*. 2013;41(2):1241-54.
23. Isel C, Munier S, Naffakh N. Experimental Approaches to Study Genome Packaging of Influenza A Viruses. *Viruses*. 2016;8(8):218.

24. Cobbin JC, Ong C, Verity E, Gilbertson BP, Rockman SP, Brown LE. Influenza virus PB1 and neuraminidase gene segments can cosegregate during vaccine reassortment driven by interactions in the PB1 coding region. *Journal of virology*. 2014;88(16):8971-80.
25. Gilbertson B, Zheng T, Gerber M, Printz-Schweigert A, Ong C, Marquet R, Isel C, Rockman S, Brown L. Influenza NA and PB1 Gene Segments Interact during the Formation of Viral Progeny: Localization of the Binding Region within the PB1 Gene. *Viruses*. 2016;8(8).
26. Kawakami E, Watanabe T, Fujii K, Goto H, Watanabe S, Noda T, Kawaoka Y. Strand-specific real-time RT-PCR for distinguishing influenza vRNA, cRNA, and mRNA. *J Virol Methods*. 2011;173(1):1-6.
27. Neumann G, Watanabe T, Ito H, Watanabe S, Goto H, Gao P, Hughes M, Perez DR, Donis R, Hoffmann E, Hobom G, Kawaoka Y. Generation of influenza A viruses entirely from cloned cDNAs. *Proc Natl Acad Sci U S A*. 1999;96(16):9345-50.

28. Alvarez DE, Lodeiro MF, Luduena SJ, Pietrasanta LI, Gamarnik AV. Long-range RNA-RNA interactions circularize the dengue virus genome. *Journal of virology*. 2005;79(11):6631-43.
29. Bak G, Han K, Kim K-s, Lee Y. Electrophoretic mobility shift assay of RNA-RNA complexes. *Methods Mol Biol*. 2015;1240:153-63.
30. Buchmueller KL, Webb AE, Richardson DA, Weeks KM. A collapsed non-native RNA folding state. *Nature Structural Biology*. 2000;7:362.
31. Sinck L, Richer D, Howard J, Alexander M, Purcell DFJ, Marquet R, Paillart J-C. In vitro dimerization of human immunodeficiency virus type 1 (HIV-1) spliced RNAs. *RNA (New York, NY)*. 2007;13(12):2141-50.
32. R Core Team. R: A Language and Environment for Statistical Computing. Available from: <https://www.R-project.org/2018>.
33. Lorenz R, Bernhart SH, Höner Zu Siederdisen C, Tafer H, Flamm C, Stadler PF, Hofacker IL. ViennaRNA Package 2.0. *Algorithms Mol Biol*. 2011;6:26-.

34. Fang XW, Golden BL, Littrell K, Shelton V, Thiyagarajan P, Pan T, Sosnick TR. The thermodynamic origin of the stability of a thermophilic ribozyme. *Proceedings of the National Academy of Sciences*. 2001;98(8):4355.
35. Misra VK, Draper DE. The linkage between magnesium binding and RNA folding. *Journal of molecular biology*. 2002;317(4):507-21.
36. Laing C, Schlick T. Computational approaches to RNA structure prediction, analysis, and design. *Current Opinion in Structural Biology*. 2011;21(3):306-18.
37. Solomatin SV, Greenfield M, Chu S, Herschlag D. Multiple native states reveal persistent ruggedness of an RNA folding landscape. *Nature*. 2010;463(7281):681-4.
38. Woodson SA. Taming free energy landscapes with RNA chaperones. *RNA Biology*. 2010;7(6):677-86.
39. Woodson SA. Compact Intermediates in RNA Folding. *Annual Review of Biophysics*. 2010;39(1):61-77.

40. Weeks KM. Protein-facilitated RNA folding. *Current opinion in structural biology*. 1997;7(3):336-42.

41. Noda T, Sugita Y, Aoyama K, Hirase A, Kawakami E, Miyazawa A, Sagara H, Kawaoka Y. Three-dimensional analysis of ribonucleoprotein complexes in influenza A virus. *Nat Commun*. 2012;3:639.

Figure Legends

Figure 1. *In vitro* RNA binding of viral RNAs (vRNAs) of H3N2 Udorn and H1N1 WSN viruses. (a) Upper and middle panels, PB1 and NA vRNAs of Udorn and WSN, respectively; lower panel, HA and M vRNAs of H1N1 WSN virus. (b) Quantification of binding shown in panel a.

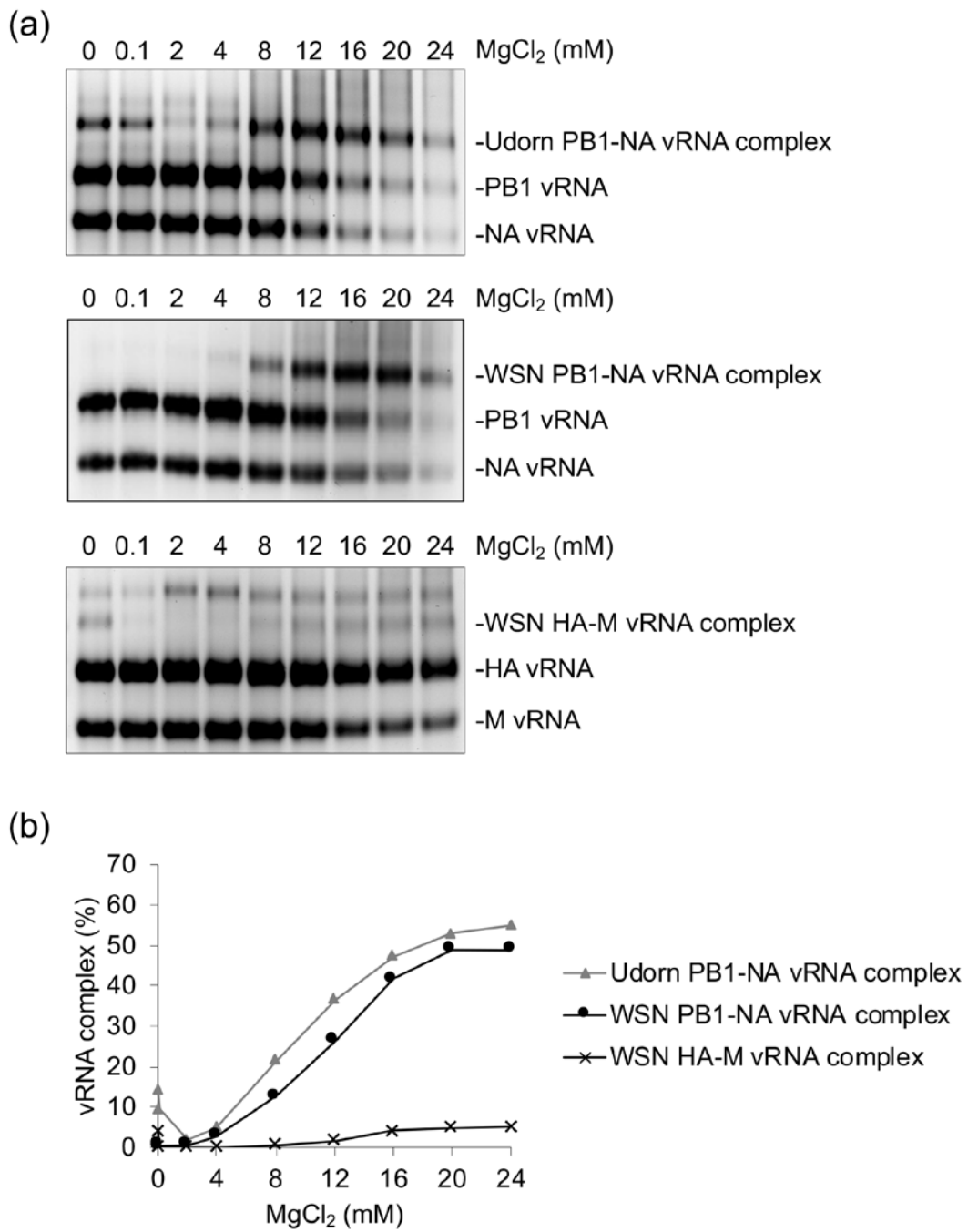
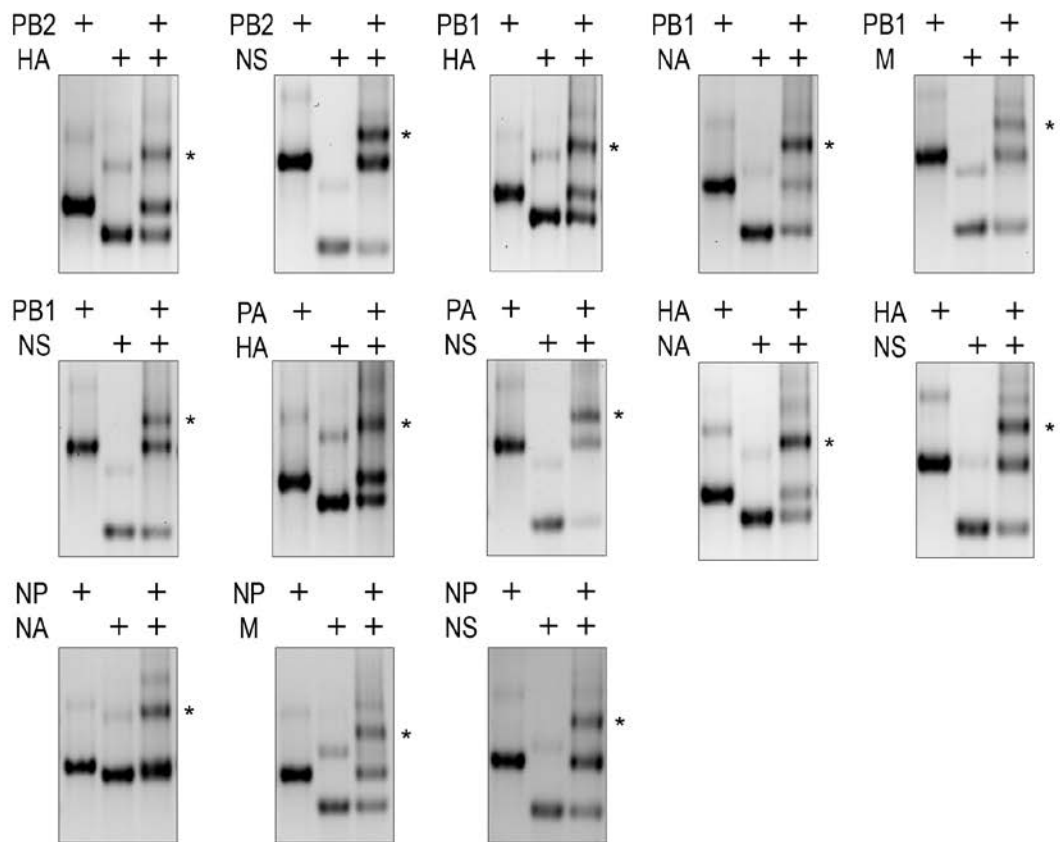


Figure 2. *In vitro* inter-segment interactions of full-length viral RNAs (vRNAs) of the H1N1 WSN virus. (a) Binding between 13 pairs of H1N1 WSN vRNAs that exhibited binding. The remaining combinations that did not form inter-segment complexes are presented in Supplementary Figure 1. Asterisks indicate the inter-segment complexes. (b) Quantification of inter-segment complex formation. Proportions are expressed as means ($n = 2$). Homodimer combinations have a black background ($n = 7-9$). Combinations showing significant heterodimer formation relative to homodimer formation of M vRNA are shown with gray backgrounds.

(a)

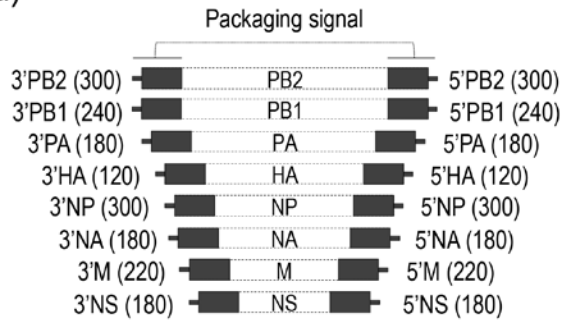


(b)

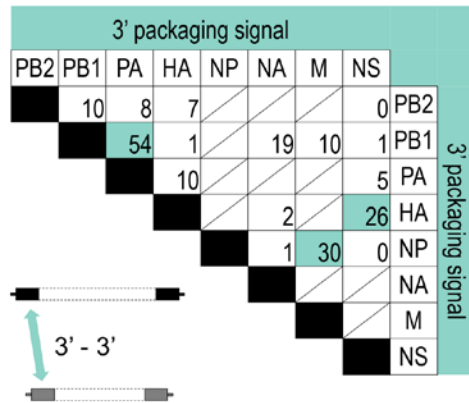
PB2	PB1	PA	HA	NP	NA	M	NS	vRNA
4	14	18	32	6	16	11	38	PB2
	2	18	38	14	48	28	24	PB1
		6	35	12	20	17	54	PA
			13	13	55	7	33	HA
				3	27	28	27	NP
					4	16	9	NA
						18	19	M
							8	NS

Figure 3. *In vitro* interactions between vRNAs through their 3'- and 5'-terminal region which contain genome packaging signals. (a) Diagram of 16 *in vitro*-transcribed short vRNA constructs. Packaging signals containing terminal non-coding and adjacent coding regions are colored dark gray. Nucleotide lengths of the respective coding regions are shown in brackets. (b, c, and d) Quantification of the complex formation between pairs of short vRNAs. Proportions of RNA–RNA complex formation, for which data are presented in Supplementary Figure 2, are indicated and those above 20% are highlighted; interactions between the 5'- (b) or 3'- (c) ends of the genome packaging signal regions from two distinct vRNAs are shaded purple and green, respectively. (d) Interactions between the 5'- and 3'-ends of genome packaging signal regions from two distinct vRNAs are shaded red.

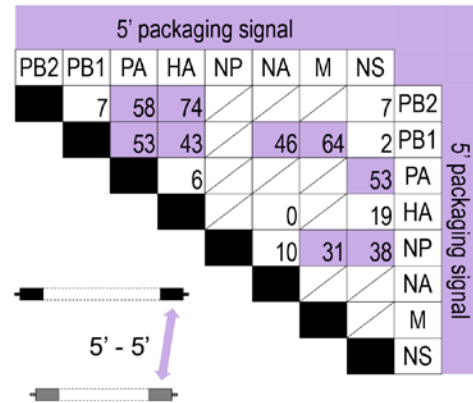
(a)



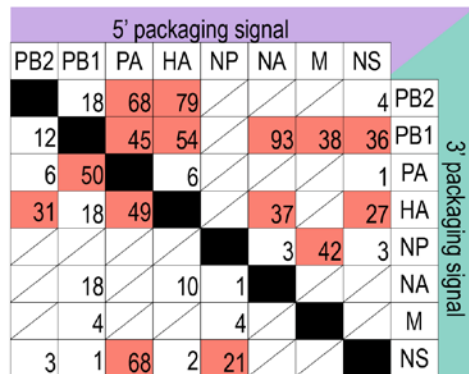
(b)



(c)



(d)



List of abbreviations

NP: nucleoprotein

Udon: A/Udon/307/72 (H3N2)

vRNP: viral ribonucleoprotein complex

vRNA: viral RNA

WSN: A/WSN/33 (H1N1)

Supporting Information

Supplemental Figure legends

Figure S1. Binding assays for 15 pairs of *in vitro*-transcribed H1N1 WSN vRNAs that did not form significant inter-segment complexes. Different combinations of the vRNA pairs were co-incubated and electrophoresed on 1% agarose gels. Asterisks indicate inter-segment complexes.

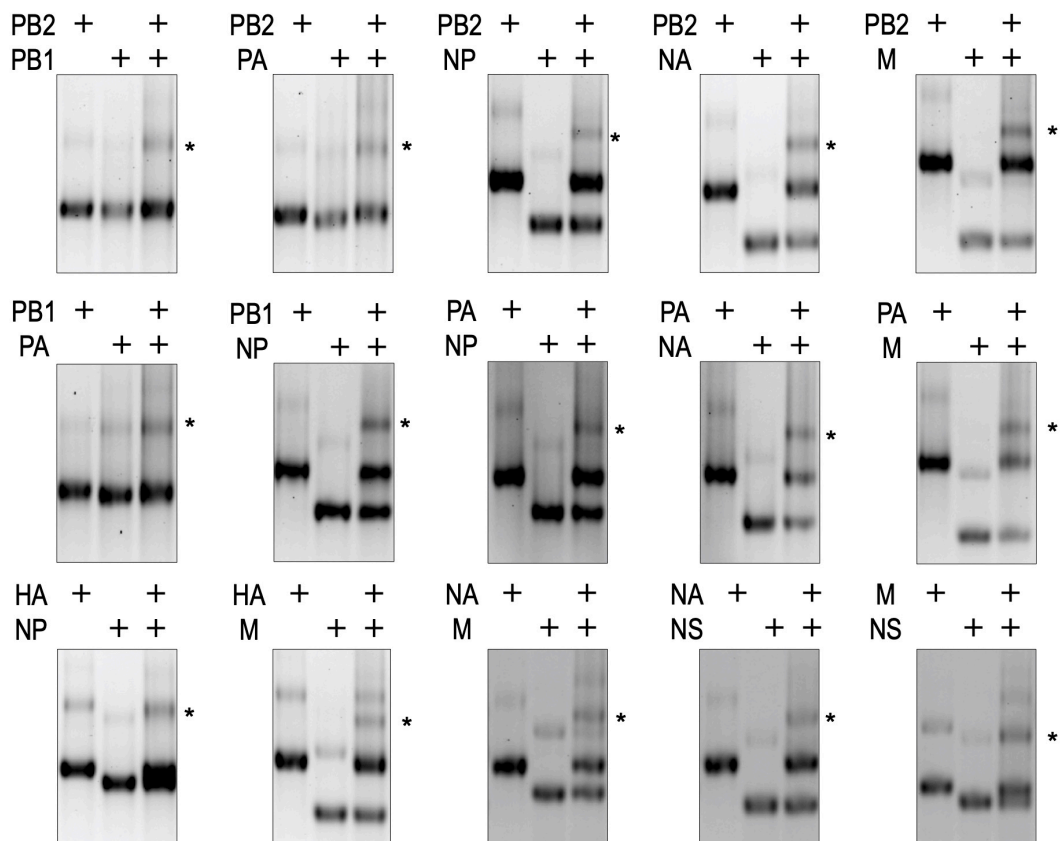
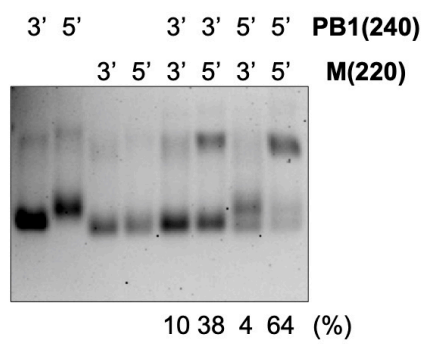
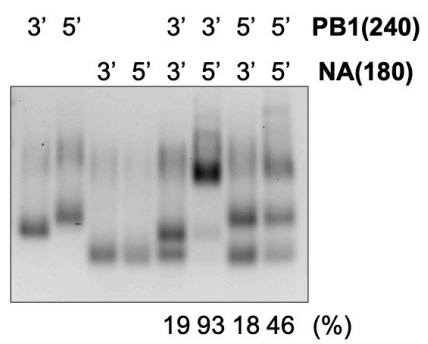
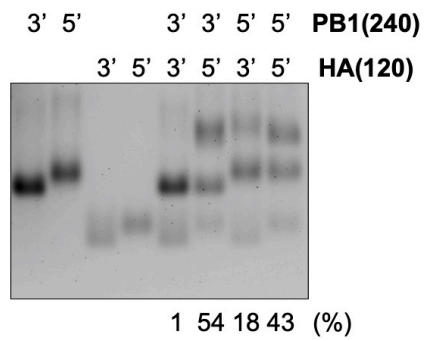
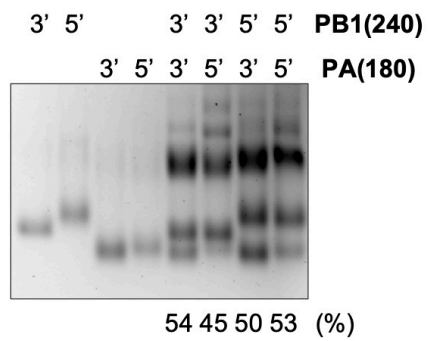
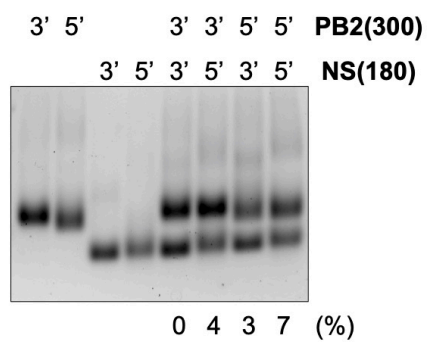
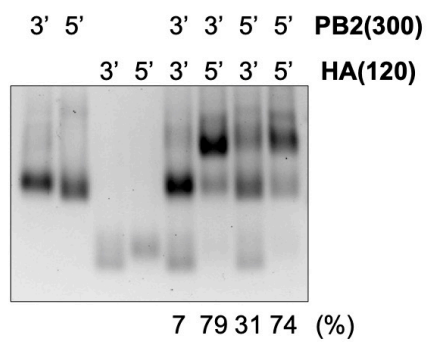
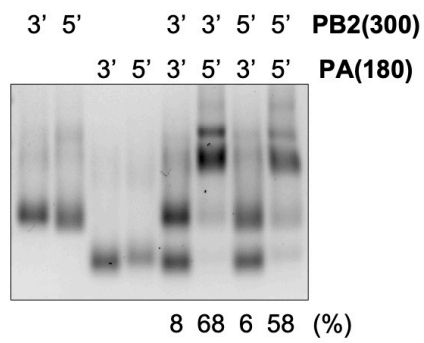
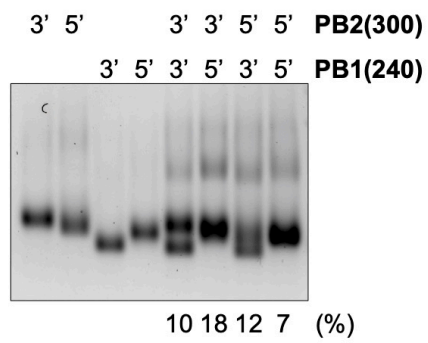


Figure S2. *In vitro* RNA binding assays using the 3'- and 5'- terminal regions containing genome packaging signals. Different combinations of *in vitro*-transcribed short vRNA pairs of the WSN strain were co-incubated and electrophoresed on 2% agarose gels. The combinations of two short vRNAs from two different vRNAs are indicated at the top of the gels. Proportions of the heterodimer formation are shown at the bottom of the gels.



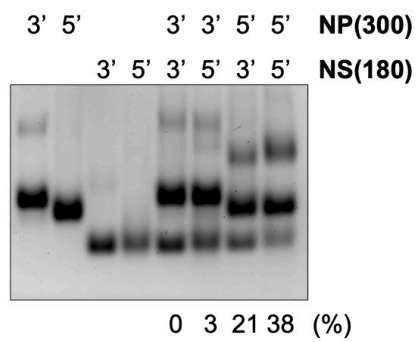
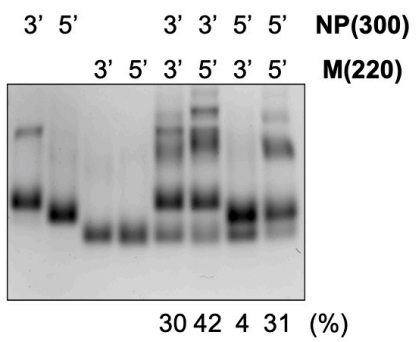
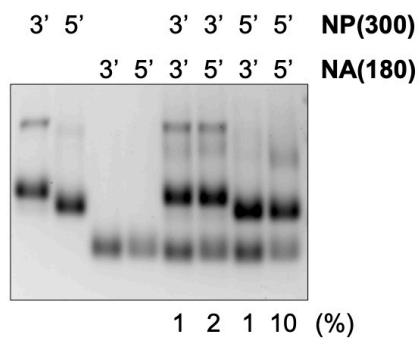
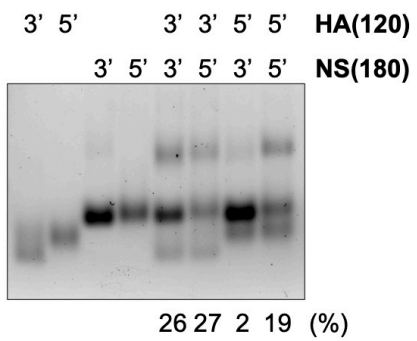
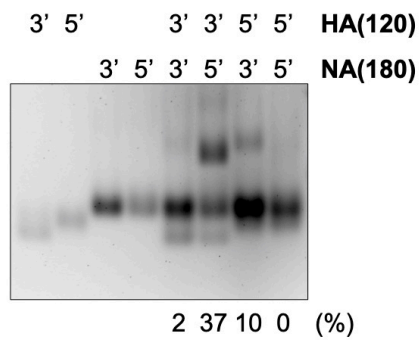
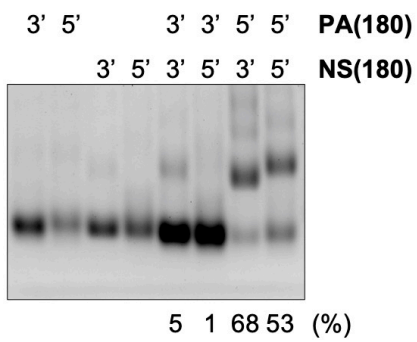
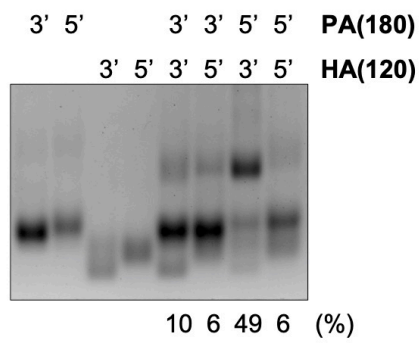
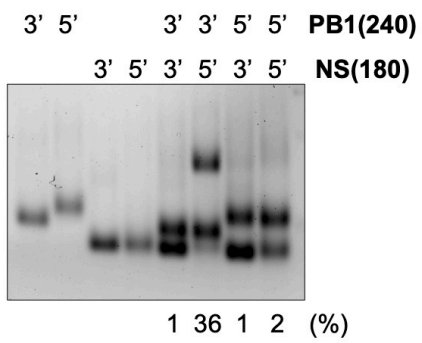
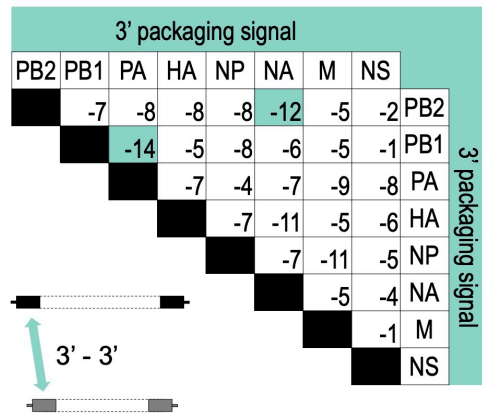
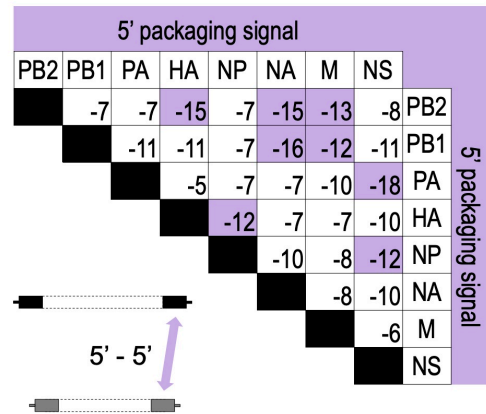


Figure S3. *In silico* predictions of vRNA–vRNA interactions through 3'- and 5'-terminal regions containing genome packaging signals. (a, b, c) Minimal free energies of complex formation between pairs of short vRNAs. Free energies less than -12 kcal/mol are highlighted; predicted interactions between the 3'- (a) or 5'- (b) ends of the genome packaging signals from two distinct vRNAs are shaded purple and green, respectively. (c) predicted interactions between the 5'- and 3'-ends of the genome packaging signals from two distinct vRNAs are shaded red. (d) Correlations between the minimal free energies of paired short vRNAs and proportions of their *in vitro* vRNA complexes are presented as a 2D histogram. The regression line (black), 95% confidence interval (gray), and Pearson correlation R-value are shown.

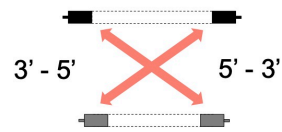
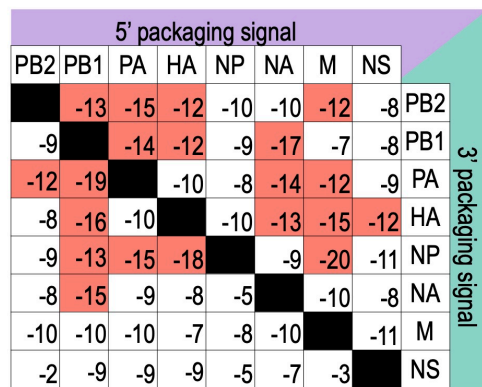
(a)



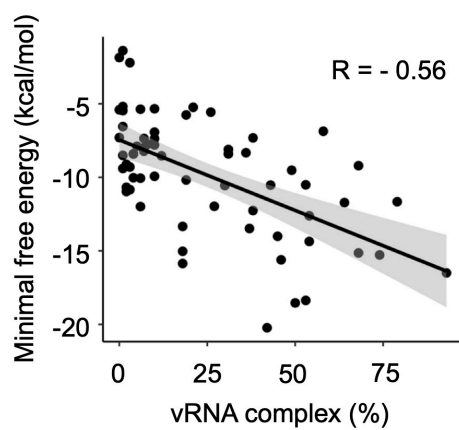
(b)



(c)



(d)



Supplemental Tables

Table S1. Primer sets for PCR used to produce templates for *in vitro* transcription of full-length vRNAs.

Name	Sequence (5' to 3')
WSNPB2_1F	AGCGAAAGCAGGTCAATTATATTCAATATGG
T7_WSNPB2_2341R	GGATCCTAATACGACTCACTATAGGGAGTAGAAACAAGGTCGTT TTTAAACTATTCG
WSNPB1_1F	AGCGAAAGCAGGCAAACCATTTGAATGG
T7_WSNPB1_2341R	GGATCCTAATACGACTCACTATAGGAGTAGAAACAAGGCATTTT TTCATGAAGGAC
WSNPA_1F	AGCGAAAGCAGGTACTGATTCAAAATGG
T7_WSNPA_2233R	GGATCCTAATACGACTCACTATAGGAGTAGAAACAAGGTACTTT TTTGGACAGTATGG
WSNHA_1F	AGCAAAGCAGGGGAAAATAAAAAC
T7_WSNHA_1775R	GGATCCTAATACGACTCACTATAGGGAGTAGAAACAAGGGTGT TTTCCTTATATTC
WSNNP_1F	AGCAAAGCAGGGTAGATAATCACTC
T7_WSNNP_1565R	GGATCCTAATACGACTCACTATAGGGAGTAGAAACAAGGGTATT TTTC
WSNNA_1F	AGCGAAAGCAGGAGTTTAAATGAATCCAAACC
T7_WSNNA_1413R	GGATCCTAATACGACTCACTATAGGGAGTAGAAACAAGGAGTT TTTGAA
WSNM_1F	AGCAAAGCAGGTAGATATTGAAAG
T7_WSNM_1027R	GGATCCTAATACGACTCACTATAGGAGTAGAAACAAGGTAGTT TTTACTCCAG
WSNNS_1F	AGCAAAGCAGGGTGACAAAGACAT
T7_WSNNS_890R	GGATCCTAATACGACTCACTATAGGAGTAGAAACAAGGGTGT TTTATTATTAATAAGC
UdornPB1_1F	AGCGAAAGCAGGCAAACCATTTGAATG
T7_UdornPB1_2341R	GGATCCTAATACGACTCACTATAGGAGTAGAAACAAGGCATTT TTCATG
UdornNA_1F	AGCAAAGCAGGAGTGAAGATG

T7_UdornNA_1 466R	GGATCCTAATACGACTCACTATAGGAGTAGAAACAAGGAGTTTT TTCTAAAATTG
----------------------	---

Table S2. Primer sets for PCR used to produce the templates for *in vitro* transcription of the short vRNAs.

Name	Sequence (5' to 3')
WSNPB2_1F	AGCGAAAGCAGGTCAATTATATTCAATATGG
T7_3'PB2(300) _R	GGATCCTAATACGACTCACTATAGGGATTCCACCATGTCACAGCC AGAG
5'PB2(300)_F	ACCACTAAAAGACTCACAGTTCTC
T7_WSNPB2_ 2341R	GGATCCTAATACGACTCACTATAGGGAGTAGAAACAAGGTCGTTTT TTAAACTATTCG
WSNPB1_1F	AGCGAAAGCAGGCAAACCATTGGAATGG
T7_3'PB1(240) _R	GGATCCTAATACGACTCACTATAGGGACTTGGTTCATTGTCTTCT GGCAGTG
5'PB1(240)_F	CAAAGAGGAATACTTGAAGATGAAC
T7_WSNPB1_ 2341R	GGATCCTAATACGACTCACTATAGGAGTAGAAACAAGGCATTTTT TCATGAAGGAC
WSNPA_1F	AGCGAAAGCAGGTACTGATTCAAAATGG
T7_3'PA(180) _R	GGATCCTAATACGACTCACTATAGGGTGACTCGCCTTGCTCATCG ATGAAGTG
5'PA(180)_F	TTTTTCAGCTGAATCAAGAAAAGTCTTC
T7_WSNPA_2 233R	GGATCCTAATACGACTCACTATAGGAGTAGAAACAAGGTACTTTTT TTGGACAGTATGG
WSNHA_1F	AGCAAAAGCAGGGGAAAATAAAAAC
T7_3'HA(120) _R	GGATCCTAATACGACTCACTATAGGGATTCTTCTCGAGTATTGTG TCAACAG
5'HA(120)_F	TATCAGATTCTGGCGATCTACTCAAC
T7_WSNHA_1 775R	GGATCCTAATACGACTCACTATAGGGAGTAGAAACAAGGGTGT TTTCCTTATATTTT
WSNNP_1F	AGCAAAAGCAGGGTAGATAATCACTC
T7_3'NP(300) _R	GGATCCTAATACGACTCACTATAGGGTACTCTCCTGTATATAGGT CCTCCAG

5'NP(300)_F	AGGGCTTCCTCGGGCCAAATCAGCATAC
T7_WSNNP_1 565R	GGATCCTAATACGACTCACTATAGGGAGTAGAAACAAGGGTATTT TTC
WSNNA_1F	AGCGAAAGCAGGAGTTTAAATGAATCCAAACC
T7_3'NA(180) R	GGATCCTAATACGACTCACTATAGGGAGCAACAAC TTTATAGGTA ATGCTG
5'NA(180)_F	GAGCTAACAGGGCTAGACTGTATG
T7_WSNNA_1 413R	GGATCCTAATACGACTCACTATAGGGAGTAGAAACAAGGAGTTTT TTGAA
WSNM_1F	AGCAAAAGCAGGTAGATATTGAAAG
T7_3'M(220) R	GGATCCTAATACGACTCACTATAGGGGTCCCCGCTCACTGGGCAC GGTGAGCGTGAAC
5'M(220)_F	TCTCGTCATTGCAGCAAATATC
T7_WSNM_10 27R	GGATCCTAATACGACTCACTATAGGAGTAGAAACAAGGTAGTTTT TTACTCCAG
WSNNS_1F	AGCAAAAGCAGGGTGACAAAGACAT
T7_3'NS(180) R	GGATCCTAATACGACTCACTATAGGGAGCACGGGTGGCTGTTTCG ATGTC
5'NS(180)_F	GGAAAATGGCGGGAACAATTAGGTCAG
T7_WSNNS_8 90R	GGATCCTAATACGACTCACTATAGGAGTAGAAACAAGGGTGT TTATTATTAAATAAGC